Ng, K. H., Tameh, E. K., & Nix, A. R. (2005). Modelling and performance prediction for multiple antenna systems using enhanced ray tracing. In Wireless Communications and Networking Conference, 2005. (Vol. 2, pp. 933 - 937). Institute of Electrical and Electronics Engineers (IEEE). 10.1109/WCNC.2005.1424633

Modelling and Performance Prediction for Multiple Antenna Systems using Enhanced Ray Tracing

K. H. Ng, E.K.Tameh and A.R. Nix

Centre for Communications Research
Merchant Venturers Building, Woodland Rd, University of Bristol, Bristol, UK

k.h.ng@bris.ac.uk, tek.tameh@bris.ac.uk, andy.nix@bris.ac.uk

Abstract: **Multiple antenna systems can enhance wireless communication links by improving their capacity and/or reliability. Multiple Input Multiple Output (MIMO) communications are the most common exploitation of this property. When applied to deterministic ray modelling, the computational cost of MIMO predication is a major drawback. In this paper, two MIMO modelling approaches are investigated. Both methods make use of an enhanced deterministic ray-tracing propagation model. The first method relies on point-to-point prediction for each of the multiple element to element links. The second approach estimates the MIMO link matrix from a single point-to-point ray tracing study. A comparison of normalized capacity and path loss is performed for the two methods in an outdoor city centre environment. For a Single Input Multiple Output (SIMO) case, the two modelling approaches are presented and compared with measured array data. Result show that the single point-to-point approximation works well and can significantly reduce run-time when compared with full element to element ray tracing.**

Keywords-ray tracing, propagation, prediction, MIMO.

I. INTRODUCTION

Multiple antenna systems that employ one or more elements at both the transmitter and receiver have the potential to greatly enhance the data capacity of a wireless communication network. The exploitation of spatial and/or temporal diversity in a MIMO (Multiple Input Multiple Output) communication system offers considerable benefit [1]. Such systems combine the modulation, coding and detection tasks to directly exploit the features present in multi-channel propagation links. Such systems generally make use of space-time and/or spatial multiplexing algorithms. The high frequency approximation of electromagnetic wave propagation based on Geometric Optics (GO) allows ray tracing to be used to predict the radio channel between any two points. This is the basis of all deterministic propagation models [2]. The major drawback of ray tracing models is their computational cost, which depends on factors such as the size and complexity of the geographic database and the interaction order in the ray search. Ray models must trade-off prediction accuracy for run-time efficiency. Nevertheless, many ray tracing models have been developed over the years and most have shown good agreement with measured channel characteristics for single antenna systems [3-4].

The conventional ray tracing model for a single antenna system performs a point to point analysis between the transmitter and receiver. For multiple antenna systems, the ray tracing operation can be performed for each and every transmitter and receiver link. This brute-force approach can be tedious and the required processing time is linearly proportional to the product of the number of transmitter and receiver elements. For most multiple antenna systems, the spacing between antenna elements is of the order of one-half wavelength. At 900 MHz, the spatial separation of elements is around 15-30cm. For higher frequencies, the separation distance reduces. Such closely spaced elements offer the possibility of exploiting spatial coherency. A multiple element channel can then be approximated using ray tracing data from a single point to point study.

This paper is organized as follows. Section II describes the single point-to-point approximation approach. Section III describes the ray tracing model and the database used in Section IV. Section IV discusses a comparison of path loss prediction using SIMO measurement data and normalized theoretic capacity for MIMO systems. The paper ends with a set of conclusions and recommendations.

II. SINGLE POINT-TO-POINT APPROXIMATION

Given that most multiple element arrays are electrically small (inter-element spacings of half a wavelength or less), spatial coherency can be exploited to avoid the need to brute force ray trace each transmit and receive element pair. Instead, the transmitter and receiver can be represented as a single virtual point. The ray tracing operation is then performed using these virtual points. The set of rays collected for each virtual point pair are then mapped to specific elements at both the transmitter and receiver. The mapping process is performed by adjusting the start and end points of each ray to the actual position of the antenna or element. For each mapped ray, a line of sight check and an electromagnetic calculation is performed. If the virtual point does not see any line of sight rays, each element must check whether a line of sight ray exists, and if it does then this ray is regenerated by the ray model. This correction is performed to ensure that high power line of sight rays are not missed by the single virtual point assumption. Each antenna or element pair shares a similar set of ray geometries. The electromagnetic properties of these rays may be different since they are recalculated based on the actual position of the given elements. Figure 1 shows the two approaches used here to analyze the multiple antenna links. Figure 1a shows the brute-force ray tracing approach for all element pairs. Figure

1b shows the virtual point approximation approach based on a simple two ray model (direct and reflected) using a two element Uniform Linear Array (ULA) at the transmitter and a single element at the receiver. The approximate approach is based on the assumption that when the virtual point is located close to the actual antenna or element position (which is true for the case of electrically small arrays), both will see a very similar set of rays. Hence, the virtual point should be located at the minimum distance from all the actual element locations in order to produce the most accurate approximation.

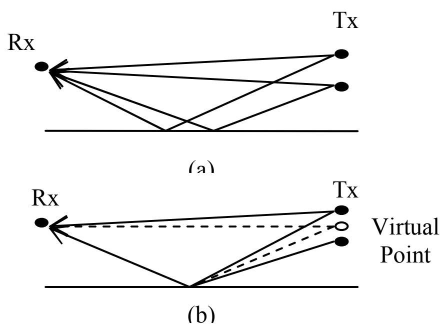

Figure 1. (a) Multiple point to point (brute force) ray tracing; (b) single point to point ray tracing approximation.

The number of rays collected from the ray tracing model is often limited by the ray power sensitivity threshold. If this is the case, the virtual antenna pattern used at the virtual point must be considered carefully. On the other hand, if raw rays generated at the virtual point are collected without considering any electromagnetic properties, then any virtual location can be used to which ray paths can be traced. When the virtual antenna pattern is used in the ray tracing process, its electromagnetic properties, such as its antenna response and polarization, will affect the number of rays generated. The geometry of the generated rays may not be similar for each of the actual antenna or element pairs. For example, if a 60 degree beamwidth directional antenna were to be used at the virtual point to represent actual elements that were omni-direction; in a simple case study we saw that more than 80% of the rays seen by the actual omni antennas were lost. If a vertically polarized virtual omni antenna were used to represent horizontally polarized real antennas then most of the rays seen by the actual antenna pair would have been rejected due to cross-polarization. Hence, an appropriate virtual antenna must be used that is highly correlated with all of the actual elements. For a ULA antenna, any of the elements can be used as the virtual antenna if the element patterns are all highly correlated. For some types of MIMO array, the element patterns may not be highly correlated, and in this case the virtual antenna pattern should be either isotropic or an approximation of the composite pattern of all elements, to ensure that no major rays are rejected. If this is the case, isotropic power ray tracing is more appropriate where polarization of the ray is ignored. At each ray interaction, only the maximum power loss (for all polarization) is considered. The only disadvantage is the extra computational time as more rays would be generated. Nevertheless, isotropic ray tracing finds all possible rays between each transmitter and receiver pair.

The advantage of using the single point-to-point approximation is its considerable computational reduction during the ray tracing stage. The process of ray path finding in ray tracing is normally the most resource consuming stage. The use of the single point-to-point approximation removes the redundancies present in performing ray tracing for each of the antenna or element pairs. Depending on the implementation used in the ray tracing stage, the reduction in computational time may be linearly proportion to the number of antenna or element pairs present in the MIMO link.

III. RAY TRACING MODEL

The ray tracing model used for the comparison analysis in Section IV is a site-specific image-based outdoor 'last mile' ray tracing model, as described in [5]. The model is capable of modelling major propagation mechanisms such as free space transmission, building reflection, building roof top and corner diffraction, building scattering and terrain scattering (plus many of their combined interactions). The model operates in a 3D vectorized environment. Various optimization techniques, such as visibility determination, object space partitioning, pre-creation of diffraction trees, and grid computing have been implemented in the model to enhance its processing efficiency. The ray tracing model is able to support both the brute force multiple point-to-point ray tracing approach and the single point-to-point approximation for multiple antenna systems. A 1km by 1km area in the centre of Bristol is used as the ray tracing database for the comparison analysis in Section IV. This database is shown (partly) in Figure 2. Building and foliage is represented as flat-topped vectorized polygonal objects. Terrain is sampled at 10m resolution. The database consists of 995 buildings, 174 foliage objects, 12,495 building polygons, 7,921 building vertical edges and 14,046 terrain pixels.

IV. COMPARISONS IN SIMULATED MIMO SYSTEMS AND WITH URBAN SIMO MEASUREMENTS

A. MIMO System

A MIMO ray tracing trial was performed with a single basestation (Tx) and 2052 mobile terminals (Rx), as shown in Figure 2. The analysis assumes a bandwidth of 20MHz at a centre frequency of 1.92GHz, with a frequency resolution of 20 kHz. The ray engine considers up to 4^{th} order reflection, 2^{nd} order diffraction, 1^{st} order building scatter and 1^{st} order terrain scatter. A power sensitivity threshold of -100 dB is used (defined as the free space loss - 100dB) since this was considered low enough to capture all major rays. The basestation is located 18m above the ground. The mobile terminals are located at 1.7m above the ground. A four element Uniform Circular Array (UCA) is assumed at the transmitter with patch elements placed at a radius of 0.3536λ. Two receiver trial scenarios are considered. In scenario A, a four element UCA is assumed with monopole elements placed around a radius of 0.3536λ. In scenario B, a four element Uniform Linear Array (ULA) with monopole elements of 0.5λ element spacing is assumed. The bore-sight of the ULA is directed randomly around the azimuth plane. Both scenarios result in a 4x4 MIMO system.

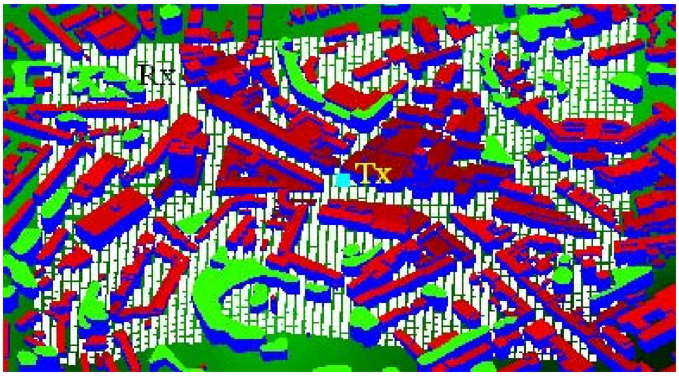

Figure 2. MIMO ray tracing trial.

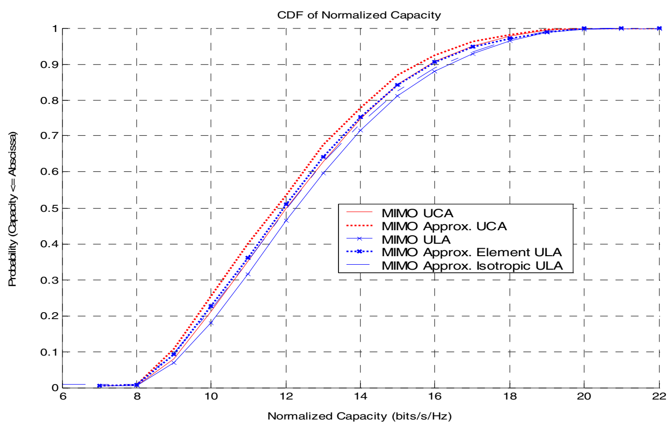

Figure 3. Comparison of normalized capacity.

TABLE I. STATISTICAL SUMMARY OF N.CAPACITY ERROR

	Mean Error (bits/s/Hz)	Std. Dev. (bits/s/Hz)	Correlation
UCA	0.56	0.81	0.94
ULA Isotropic	0.46	0.74	0.96
ULA Element	0.53	0.91	0.93

TABLE II. STATISTICAL SUMMARY OF PATH LOSS ERROR

	Mean Error (dB)	Std. Dev. (dB)	Correlation
UCA	0.84	1.82	0.99
ULA Isotropic	0.83	1.56	0.99
ULA Element	0.85	1.82	0.99

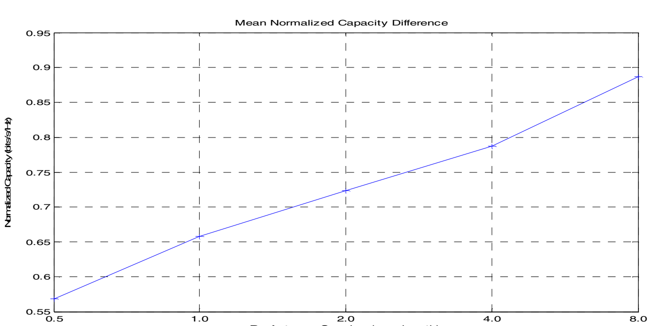

Figure 4. Comparison of normalized capacity error for different antenna spacings.

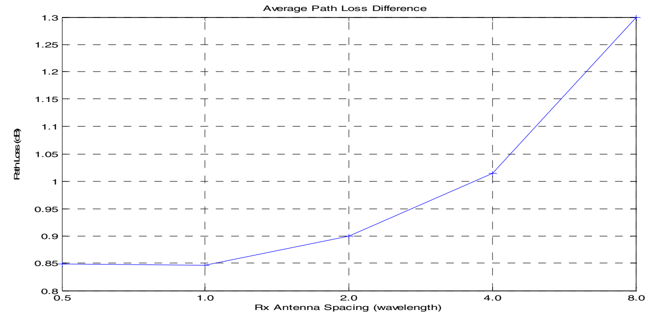

Figure 5. Comparison of average path loss error for different antenna spacing.

Comparisons are now made for both scenarios using the brute force and virtual antenna approach. Isotropic ray tracing is compared with the use of a virtual antenna in Scenario B only. The brute force multiple point-to-point approach is denoted by 'MIMO'. The virtual antenna single point-to-point approximation is denoted by 'MIMO Approx.'. Figure 3 shows a cumulative distribution function comparison of the predicted instantaneous normalized MIMO capacity for a fixed Signal-to-Noise ratio (SNR) of 20dB. The statistical results of normalized capacity and average path loss are shown in Table I and Table II respectively. Note that these errors are calculated as absolute value.

From Figure 3 and Table I, it can be seen that the normalized capacity difference for both the MIMO and MIMO approximation is about 0.5 (bits/s/Hz) for all cases. The MIMO approximation approach predicts a lower capacity level compared to the true MIMO approach. The capacity of a MIMO system is dependent on the correlation between the transmission coefficients [6]. When the transmission coefficients have a low level of correlation, large capacity gains are possible. Since a similar set of rays is being used for each transmission sub channel in the MIMO approximation method, even given the re-adjustment of the start and end point of each ray, the correlation of the ray set for each transmission sub channel is higher than the ray set produced by the exact multiple point-to-point ray trace. Hence the MIMO approximation results in a lower capacity prediction when compared to the exact approach. From Table II, it can be seen that the mean error for the path loss prediction for both approaches is less than 1dB. For the case of the ULA, although both the isotropic and the element ray tracing approximation methods gave similar results, a reduction in computational time of 20% was seen with the element ray tracing approach. It should be noted that all processing times were based on a standard Windows P4 2.4GHz processor.

A comparison of the mean normalized capacity error and path loss error with different UCA element spacing for Scenario A is shown in Figures 4 and 5. It can be seen that the errors are proportional to the element spacing. A comparison of computational time for different numbers of element in the UCA is also made in scenario A, except that the transmitter now uses an omni antenna. Figure 6 shows that the computational time using the approximation is greatly reduced when compared to the brute force method. As an example, for 8 elements the computational time of the brute force method is around 456% of the approximation method.

 0-7803-8966-2/05/$20.00

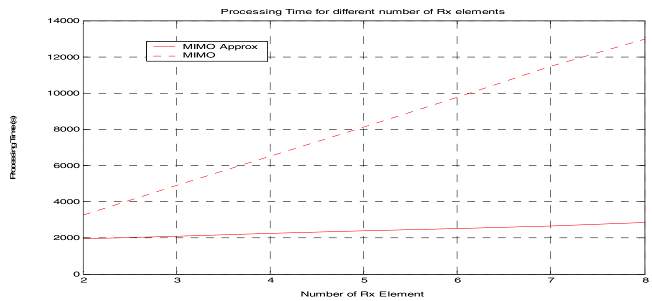

Figure 6 Comparison of computational time different number of elements.

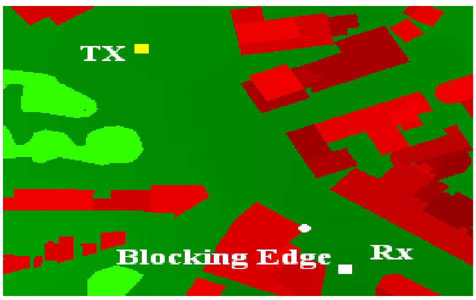

Figure 7. Trial Map for near edge scenario.

TABLE III. NORMALIZED MIMO CAPACITY PREDICTION

Methods	Scenario A	Scenario B
Brute-force	18.6	15.7
Approx.(w/o LOS)	16.3	18.2
Approx (w LOS)	16.1	15.5

The error between the true MIMO approach and the MIMO approximation occurs due to the difference in the number of rays seen by the actual antenna and the virtual antenna. The error may be significantly large in the case where some of the elements are shadowed, and there is no line of sight (LOS) between the virtual antenna pair. This would result in a large power prediction in the true MIMO approach and a low power prediction in the MIMO approximation approach because of the missing LOS rays. On the other hand, if the virtual antenna sees the LOS, but some of the element links pairs do not, then these LOS rays would be removed in the normal procedure as described in Section II. These scenarios are common when an antenna array is in close proximity to a building edge, as illustrated in Figure 7. From Figure 7, an eight element UCA antenna (basestation) is placed 3m above the ground and a mobile antenna (also an eight element UCA) is placed 1.7m above the ground. Two scenarios are now considered here, referred to as Scenarios A and B. In scenario A, the basestation virtual antenna is placed in a line of sight location. In scenario B, the mobile virtual antenna is placed in a non-line of sight location. When the true UCA is used in both of these scenarios, some of the elements would see a line of sight, while some would be blocked by the building edge, as shown in Figure 6. A comparison of the instantaneous normalized MIMO capacity using 1) the multiple point-to-point method, 2) the MIMO approximation method without the use of self-generated LOS rays, and 3) the MIMO approximation method with self-generated LOS rays is now studied for both scenarios. The term 'self generating LOS ray' refers to the process of regenerating LOS rays when the virtual antenna pairs do not have LOS, as described in Section II. The results are given in Table III. In scenario A, both MIMO approximation methods produce similar results since they share the similar LOS rays from the virtual antenna. However, in scenario B, one would expect significant error due to the missing LOS rays for the MIMO approximation case without self-generated rays. From Table III, an extra capacity error of 2.5 bits/s/Hz is produced and this shows the importance of re-checking and regenerating the LOS rays in the MIMO approximation method.

B. SIMO System

The true and approximate multiple element approaches are now used for a SIMO trial and both results are compared with outdoor SIMO measurements in the centre of Bristol. The basestation is mounted on a building top (approx. 30m from the ground) and 400 receiver points are placed along the three routes shown in Figure 8 (approx. 1.7m from the ground). An eight element ULA with +45 polarization is used at the basestation and a single omni-direction antenna is used at the mobile terminal. Reflection is performed up to the fourth order, diffraction up to the second order, and terrain scattering is also considered. A bandwidth of 20MHz at a centre frequency of 1.92GHz is assumed, with a frequency resolution of 156.25 kHz. For the SIMO approximation approach, the same $+45^0$ polarized single ULA element is used as the virtual antenna and this is positioned at the centre of the actual ULA.

Figure 8. SIMO trial map.

Figure 9 shows a comparison of the path loss prediction for this SIMO trial. A statistical summary is also shown in Table IV. It can be seen that the SIMO approximation approach gives similar prediction accuracy to the true SIMO approach, with a negligible difference between the two cases (0.04dB for the mean error).

Although the measurement trial provided here is for path loss, and no comparison of capacity is available, it is possible to compare the complex correlation transmission coefficients. Since the capacity of a MIMO system is dependent on the transmission correlation coefficients, a comparison of the autocorrelation of the transmission coefficients will provide an indication of the potential accuracy of a MIMO capacity prediction. For each basestation to mobile terminal antenna pair, there are 8x1 transmission sub channels. An 8x8 correlation matrix, with element CM_{ij} is defined such that each element *i,j* is the correlation coefficient between transmission sub channel *i* and *j*. The Mean Correlation Error Matrix (CEM) is the mean of the difference between the correlation matrix from the measurement and the corresponding predicted value. The Standard Deviation Correlation Error Matrix is the standard deviation of the difference between the measured correlation matrix and the measurement value. Figure 10 shows the Mean CEM and Standard Deviation CEM for the SIMO and SIMO approximation case. The 16x16 matrix is arranged in such a way that each 8x8 quadrant, starting from the top left in a clockwise manner, is given as the mean CEM and the STD of the CEM for the SIMO case, and the STD of the CEM and the mean CEM for the SIMO approximation case respectively. Table V shows the statistical average of all the correlation coefficient values in all CEMs.

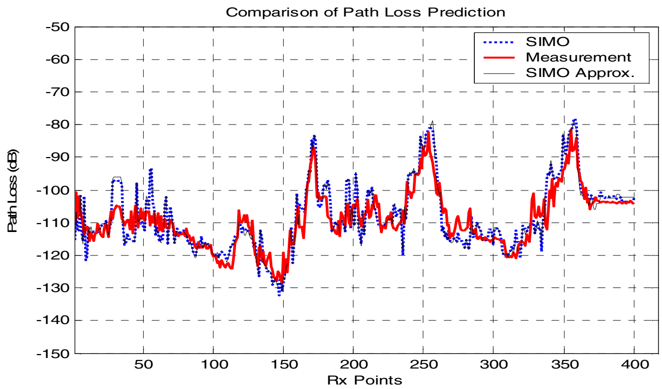

Figure 9. Comparison of SIMO path loss prediction.

TABLE IV. STATISTICAL SUMMARY OF PATH LOSS PREDICTION

	Mean Error (dB)	Std. Dev. (dB)	Correlation
SIMO	3.6520	3.0903	0.8544
SIMO Approx.	3.6962	3.1213	0.8533

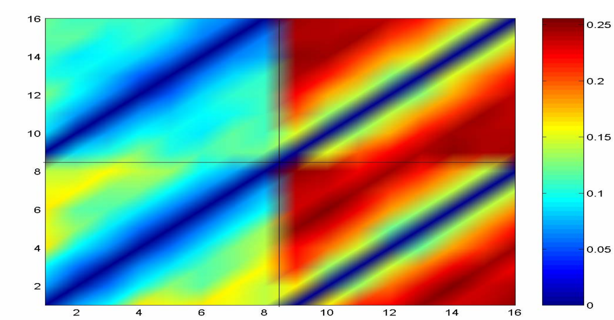

Figure 10. Correlation Error Matrix.

TABLE V. AVERAGE OF MEAN CORRELATION ERROR MATRIX AND STANDARD DEVIATION CORRELATION ERROR MATRIX

	Mean CEM	Std. Dev. CEM
SIMO	0.08	0.18
SIMO Approx.	0.10	0.18

From Figure 10, it can be seen that both the SIMO and the SIMO approximation cases produce higher correlation values than the measurement data for larger element spacings (at the top left and bottom right of each quadrant). Nevertheless, the error is low with a mean correlation error of just 0.08 for the SIMO case and 0.10 for SIMO approximation, as shown in Table V. The SIMO approximation produced additional correlation errors, however these are small and for most cases can be considered negligible compared to the true SIMO approach. The processing time for the true SIMO approach is approximately 6hrs and 16 minutes, while for the SIMO approximation it is around 40 minutes. In this case, the SIMO approximation has reduced the run time by a factor of 9 times.

V. CONCLUSIONS

Two different approaches to implementing multiple antenna systems in a ray tracing model have been explored and discussed. One approach used a brute force method to perform multiple point-to-point studies, while the second method used a single point-to-point approximation using virtual antennas at the basestation and mobile terminal. A comparison of both schemes was performed for a simulated MIMO system and for a measured outdoor urban SIMO link. Results have shown that the single point-to-point approximation works well in most cases and produces a negligible additional prediction error. The run time saving using this approximation is considerable, with a factor approaching 10 seen in these studies. We conclude that multiple antenna approximation techniques can work well so long as the arrays are electrically small and a suitable virtual antenna is used.

ACKNOWLEDGEMENTS

This work was performed under the IST-2001-32549 ROMANTIK project. The authors would like to thank Prof. Mark Beach, Mythri Hunukumbure and Sze Ern Foo for performing the channel measurements used in this study

REFERENCES

[1] G. J. Foschini, "Layered space-time architecture for wireless communication in a fading environment when using multi-element antennas," *Bell Labs Techn. J.*, pp. 41–59, Autumn 1996.

[2] D. A. McNamara, C. W. I. Pistorius, and J. A. G. Malherbe, *Introduction to the Uniform Geometrical Theory of Diffraction. Norwood, MA: Artech House, 1990.*

[3] G.E. Athanasiadou, A.R.Nix and J.P.McGeehan, "A microcellular ray-tracing propagation model and evaluation of its narrow-band and wide-band predictions," IEEE Journal on Selected Areas in Communications, vol 18., No.3, pp.322- 335, March 2000.

[4] K. Rizk, R. Valenzuela, S. Fortune, D. Chizhik, and F. Gardiol, " Lateral, Full and Vertical Plane Propagation in Microcells and Small Cells," in *48th IEEE International Conference on Vehicular Technology (VTC)*, pp. 998-1003, May 1998.

[5] K. Ng, E. Tameh and A. Nix, "An Advanced Multi-Element Microcellular Ray Tracing Model," in Proc. of *1st International Symposium on Wireless Communication Systems 2004,* to be published.

[6] D. Shiu, G. Foschini, M. Gans, and J. Khan, "Fading correlation and Its Effect on the Capacity of Multielement Antenna Systems," *IEEE Trans on Communications,* vol. 48, pp.502-513, March 2000.

[7] S. E. Foo, M. A. Beach, P. Karlsson, P. Eneroth, B. Lindmark and J. Johansson, Spatio-Temporal Investigation of UTRA FDD Channels. Proc. IEE 3G Mobile Communication Technologies 2002, pp. 175--179.